Identifying sparse connectivity patterns in the brain using resting-state fMRI

- **Journal**: NeuroImage (2015)
- **Author**: Eavani H, Satterthwaite TD, Filipovych R, Gur RE, Gur RC, Davatzikos C
- **Link**: https://www.ncbi.nlm.nih.gov/pmc/articles/PMC4262564/#!po=1.35135

Contents

Abstract

- Current methodologies assume spatial or temporal separation of the underlying networks.
- It is now increasingly evident that neural systems use parsimonious formations and functional representations to efficiently process information while minimizing redundancy.
- A parsimonious representation of brain function is **sparse connectivity patterns (SCPs)**, whose differential presence explains inter-subject variability.

Introduction

- **Functional connectivity** is defined as correlations between the spontaneous fluctuations in the fMRI time-series among different regions.
- Prior research is often based on prior knowledge of a "seed" region of interest.
- **Graph partitioning approaches**
  - do not allow for spatial overlap.
  - ignore that brain regions can participate in multiple functional networks.
  - limit their analysis to strong positive correlations.

- The **hierarchical clustering algorithm** finds nested communities but does not allow for overlaps at each level in the hierarchy.
- The notion of **"link communities"** introduced in Ahn et al. (2010) is elegantly able to handle overlaps by assigning unique membership to edges rather than nodes.
- Approaches like **correlation clustering** and the **Potts model based approach** are **partitioning approaches** which allow negative values.
- In resting state fMRI, highly negative edges imply strong **anti-correlation**, meaning these nodes express the same information, since they are strongly statistically dependent.

- **Continuous matrix factorization approaches** like principal component analysis (PCA), independent component analysis (ICA) or non-negative matrix factorization (NMF)
  - interpreted as **soft-clustering**, or a continuous relaxation of the discrete clustering problem.
  - do not suffer from issues of non-overlap and negative values.
  - the lack of interpretability of the resulting components.
  - make clustering inference difficult.
  - lack between-network interactions.

- **Connectivity based approaches** is unable to directly quantify inter-subject variability in functional connectivity.
- Source of variation across subjects
  - the average strength of networks.
  - the extent to which that functional unit is recruited in each subject.
  - an indicator of functional development or abnormality.
  - different membership of nodes to networks.

- In a **neuronal sparse coding system**, information is encoded by a small number of synchronous neurons that are selective to a particular property of the stimulus.
- **Sparse connectivity patterns (SCPs)**
  - encode system-level function.
  - each consists of a small set of spatially distributed, functionally synchronous brain regions.
  - do not necessarily need to be present in each individual or subsets of individuals.
- Sparsity-based approaches bridge the gap between discrete clustering techniques and continuous dimensionality reduction approaches.
- In this paper, the proposed method focuses on finding common networks that characterize average whole-brain functional connectivity in a group of subjects, while capturing inter-subject variations.

Identification of Sparse Connectivity Patterns

- If a correlation matrix were constructed for each of these SCPs, it would show two properties:
  - large number of edges with zero weights, or **sparsity**
  - low information content, or **rank deficiency**
- Nodes are assigned to an SCP if the strength of the edges between them co-vary across subjects.
- Model Formulation
- Optimization strategy
- Model Selection
- SCP Visualization

Model Formulation

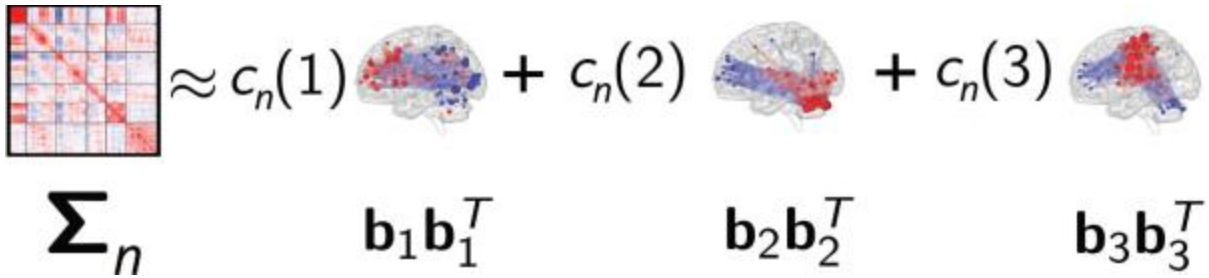

- Each vector b_k reflects the membership of the nodes to the sub-network k. If $|bk(i)| > 0$, node i belongs to the sub-network k, and if $b_k(i) = 0$ it does not.
- If two nodes in b_k have the same sign, then they are <u>positively correlated</u> and opposing sign reflects <u>anti-correlation</u>.
- l_1-norm of b_k is restricted to not exceed a constant value λ.

- Math presentation

$$\sum_n \approx \sum_{k=1}^{K} c_n(k) b_k b_k^T = B \cdot \mathrm{diag}(c_n) \cdot B^T \triangleq \hat{\sum}_n$$

- The target of optimization is

$$\min_{B,C} \sum_{n=1}^{N} || \sum_n - B \cdot \mathrm{diag}(c_n) \cdot B^T ||_F^2$$

, subject to

$$\begin{aligned} & \|\mathbf{b}_k\|_1 \leq \lambda, \quad k=1,\ldots,K, \\ - \quad & 1 \leq \mathbf{b}_k(i) \leq 1, \quad \max_i |\mathbf{b}_k(i)| = 1, \quad i=1,\ldots,P \\ & \mathbf{c}_n \geq 0, \qquad n=1,\ldots,N \end{aligned}$$

Optimization strategy

- At each iteration a local minimum is obtained using **projected gradient descent** (Batmanghelich et al., 2012).

Model Selection

- As values of K and λ are increased, the approximation error is reduced.
- Beyond a certain value of K it is likely that the model is over-fit to the data
- Two-fold cross-validation is performed, and the value at which there is no gain in generalizability (drop in error) is chosen to be the operating point.
- Test error is defined as

$$\text{Test Error} = \frac{\sum_{n=1}^{N^{test}} \left\| \Sigma_n^{test} - \mathbf{B}^{train} diag\left(\mathbf{c}_n^{test}\right) \left(\mathbf{B}^{train}\right)^T \right\|_F^2}{\sum_{n=1}^{N^{test}} \left\| \Sigma_n^{test} - \bar{\Sigma}^{test} \right\|_F^2}$$

SCP Visualization

- The resulting SCPs B are projected on to surface space using **dual-regression**.
- Time-courses are regressed against the 4D volumetric voxel wise time-series data.

Experiments on simulated data

- Generation of simulated data
- Evaluation of results for simulated data
- Results from simulated data

Generation of simulated data

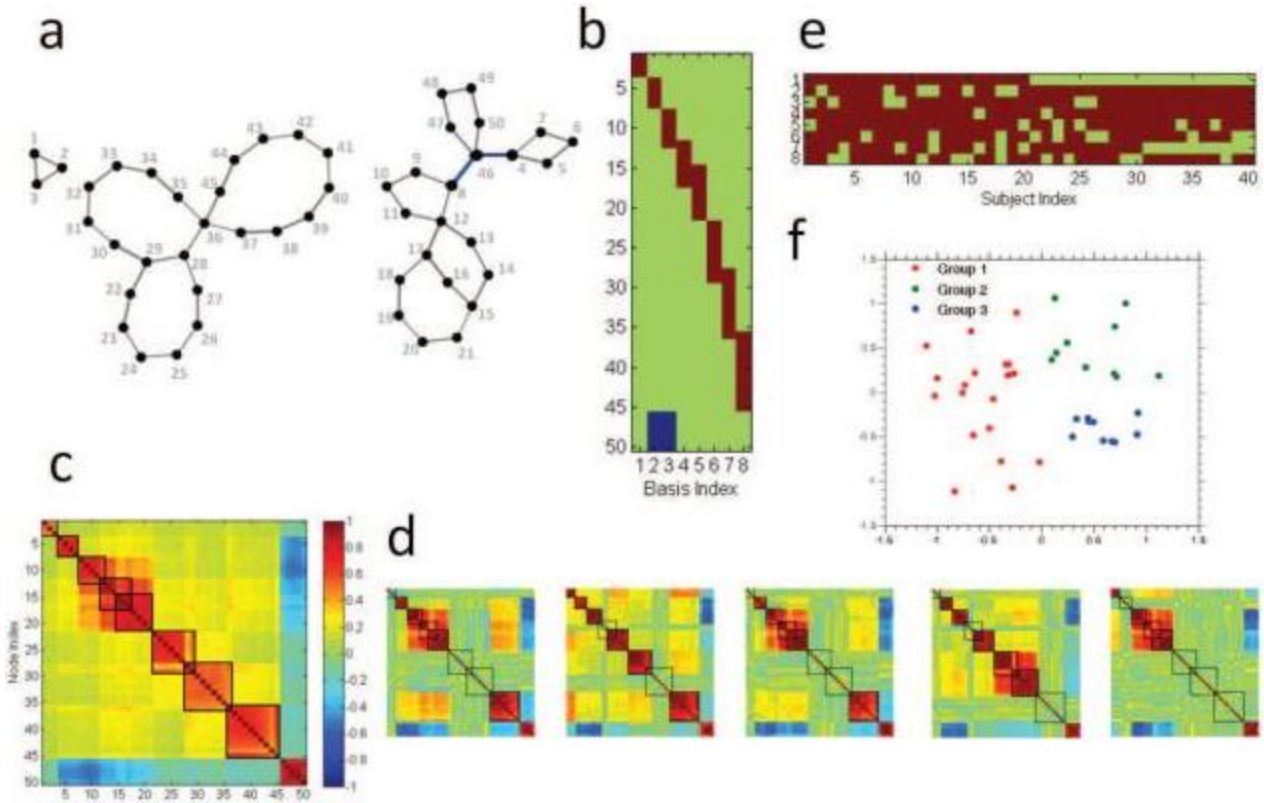

- Forty subjects is generated, each of which is associated with a fixed underlying network configuration consisting of fifty nodes.
- (Figure 2a) The network is designed in such a way that it has eight SCPs, with SCP size varying between three to ten nodes.
- (Figure 2b) Ground-truth SCP basis B^{true}.
- (Figure 2e) In each subject, networks are either "active/on" or "inactive/off", i.e. all the edges/ correlation strengths of the SCP are zero.
- NetSim (Smith et al., 2011) simulates BOLD time-series at each node.
- (Figure 2c) The subject-average correlation matrix.
- (Figure 2d) Correlation matrices of five randomly chosen subjects.

Evaluation of results for simulated data

- One-to-one matching between the two sets of vectors using the Hungarian Algorithm.
- Comparison between
  - SCPs obtained using Sparse Learning
  - sub-graphs produced using Infomap
  - TFMs generated using Temporal ICA
  - Intrinsic Connectivity Networks (ICNs) computed using Spatial ICA
- Concatenated time-series data were used as input for Temporal ICA as well as Spatial ICA.
- Dimensionality reduction was performed by running PCA before ICA.

Results from simulated data

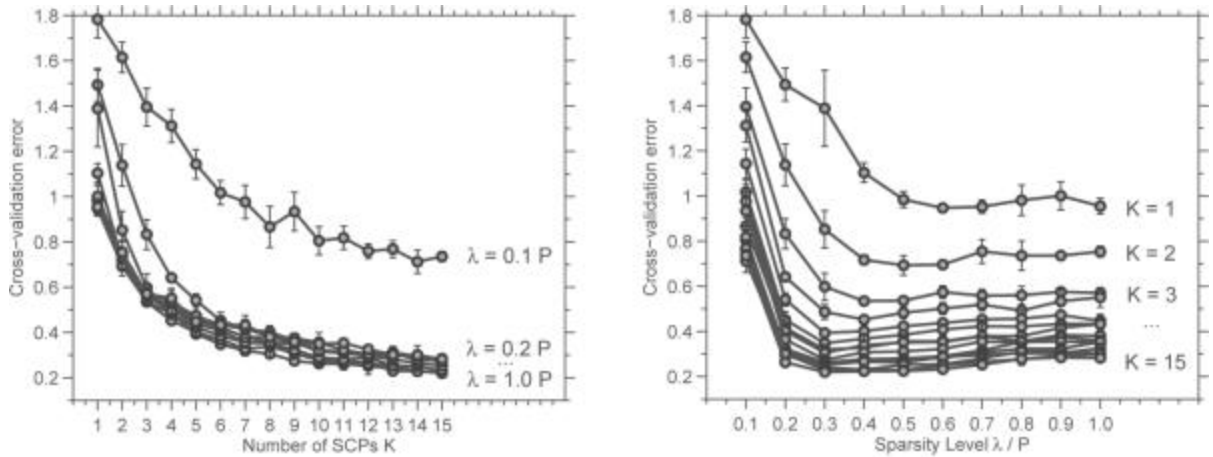

(a) Variation with K (b) Variation with λ

- It is clear that the MSE saturates beyond $\boldsymbol{\lambda}$ = 0.2.
- Choice of $\boldsymbol{K}$ is somewhat unclear.

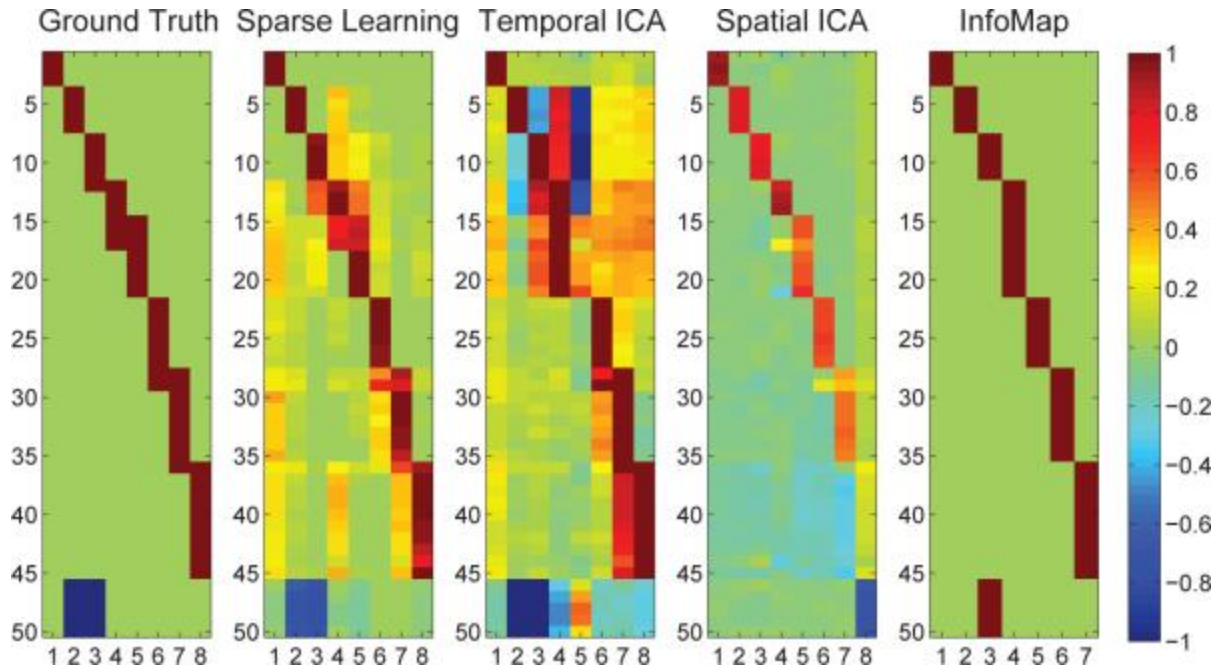

- SCPs computed using Sparse Learning are closest to the ground-truth.

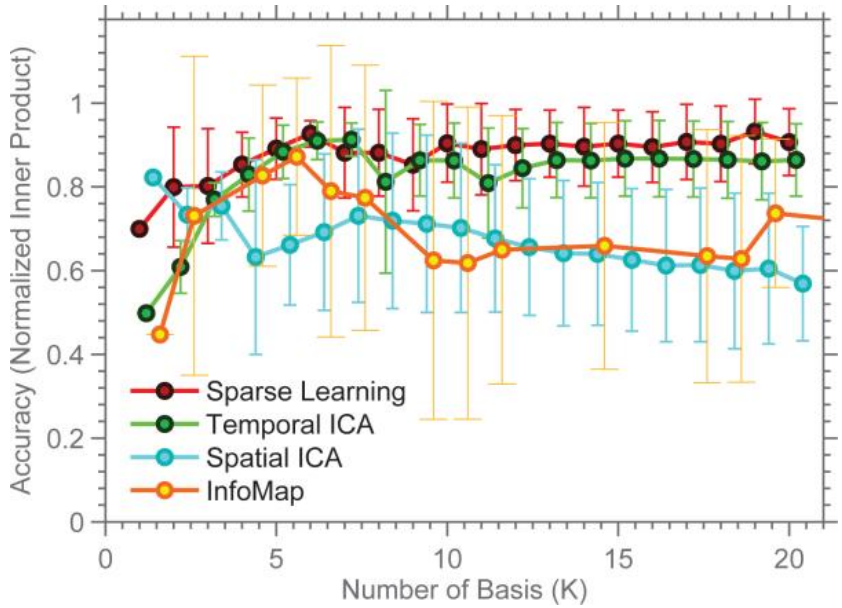

- SCPs show slightly higher accuracy than the three other methods, for all values of K.
- Temporal ICA comes a close second, as it is able to capture many of the positive/negative correlations.
- Both Spatial ICA and InfoMap produce non-overlapping ICNs/sub-graphs, and as the value of K is increased, these components get smaller/more fragmented.

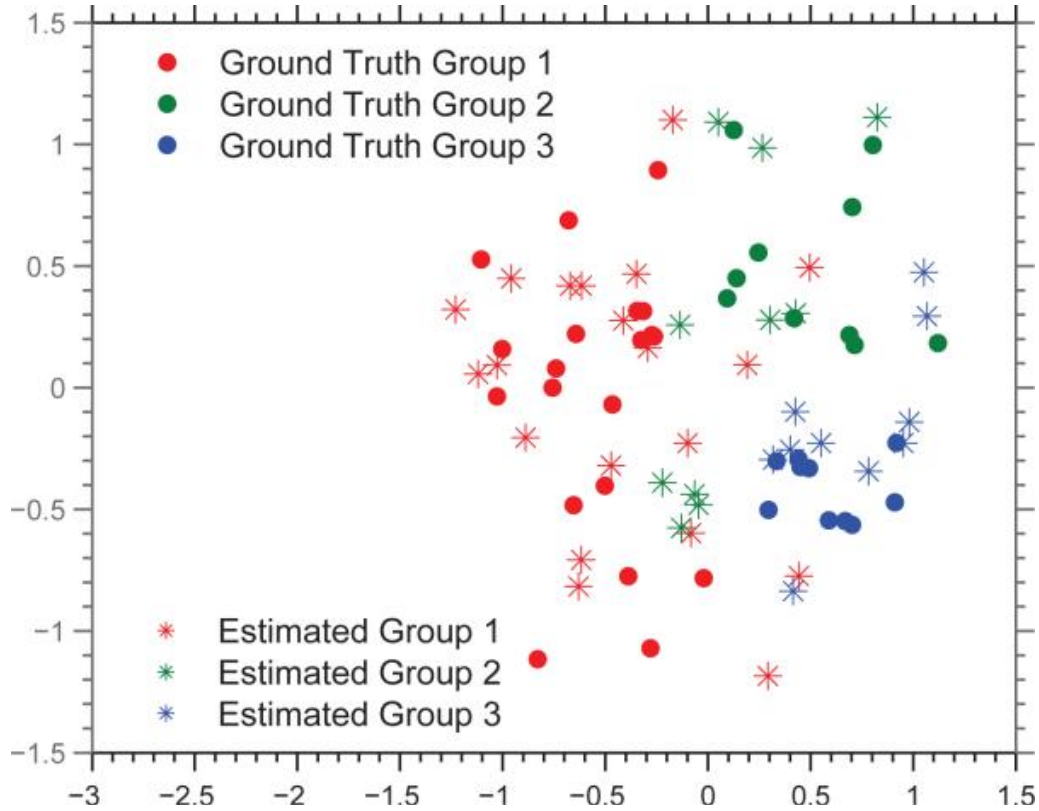

- Sparse Learning is able to capture the heterogeneity in the subject-space.

Experiments on resting state fMRI data

- Data
  - Participants
  - Data acquisition
  - Node definition
  - Registration
  - Data processing
- Evaluation of results for rsfMRI data
  - Reproducibility
  - Data fit
  - Spatial Overlap and Temporal Correlation
  - Reproducibility across datasets
- Results from rsfMRI data
  - Reproducibility and Approximation error
  - Spatial Overlap and Temporal Correlation
  - Reproducibility across datasets
  - Comparison with sub-graphs and TFMs

Node definition

- Most studies resort to dimensionality reduction, often through the use of anatomic atlases or through functional parcellation schemes.
- Nodes based on anatomic definitions often cross functional boundaries, leading to inaccurate network estimation.
- Power et al. (2011) "**areal graph**" defined 264 nodes and 34,716 unique edges.
- Based on the **discrete clustering algorithm Infomap** (Rosvall and Bergstrom, 2008), each ROI was categorized by Power et al. (2011) as belonging to one of thirteen non-overlapping sub-graphs.

Data fit

- Let B denote the set of basis vectors output by any of the four methods.
- Let $Y_n \in R^{P \times T}$ and $X_n \in R^{K \times T}$ be the subject-specific time-series and basis-specific time-series respectively.
- Correlation data fit is defined as $\sum_{n=1}^{N} || \sum_n - \hat{\sum}_n ||_F^2$, where

$$\begin{aligned} \hat{\Sigma}_n &= \mathbf{B} \quad diag\,(\mathbf{c}_n) \quad \mathbf{B}^T && \text{for Sparse Learning} \\ &= \mathbf{B} \quad \mathbf{X}_n \quad \mathbf{X}_n^T \quad \mathbf{B}^T && \text{for InfoMap, Spatial and Temporal ICA} \end{aligned}$$

- Time-series data fit is defined as $\sum_{n=1}^{N} ||Y_n - B \cdot X_n||_F^2$

Spatial Overlap and Temporal Correlation

- Spatial overlap is defined as

$$\text{Spatial Overlap} = \sum_{i,j=1,i\neq j}^{K} \frac{|\mathbf{b}_i|^T |\mathbf{b}_j|}{\|\mathbf{b}_i\|_2 \|\mathbf{b}_j\|_2}$$

- Temporal correlation is defined as

$$\text{Temporal Correlation} = \sum_{n=1}^{N} \sum_{i,j=1,i\neq j} \frac{\mathbf{x}_{ni}^T \mathbf{x}_{nj}}{\|\mathbf{x}_{ni}\|_2 \|\mathbf{x}_{nj}\|_2}$$

Results from rsfMRI data

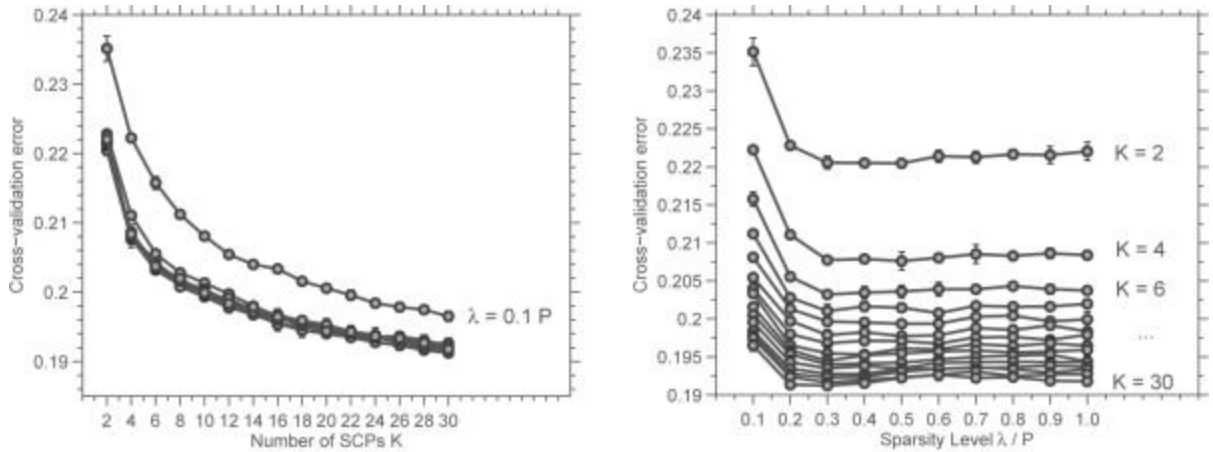

(a) Variation with K (b) Variation with λ

- Sparse Learning was run on the entire sample of 130 subjects with the values K = 10, λ = 0.3.

- Dorsal Attention SCP

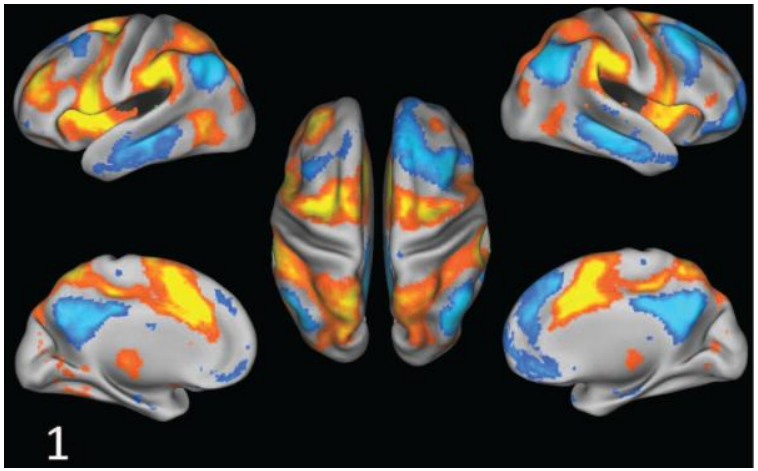

- Executive Control SCPs

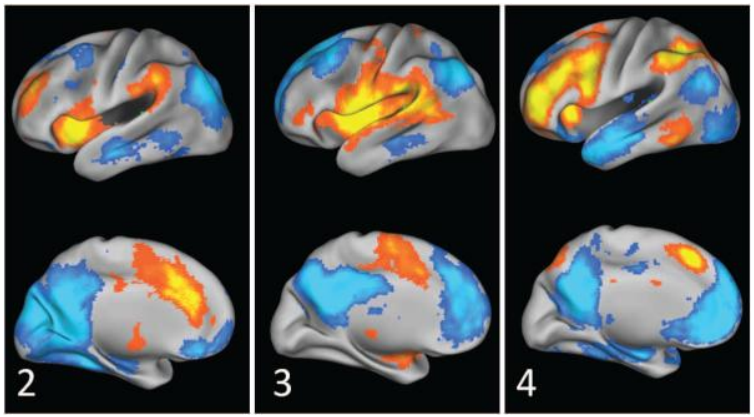

- Motor SCPs

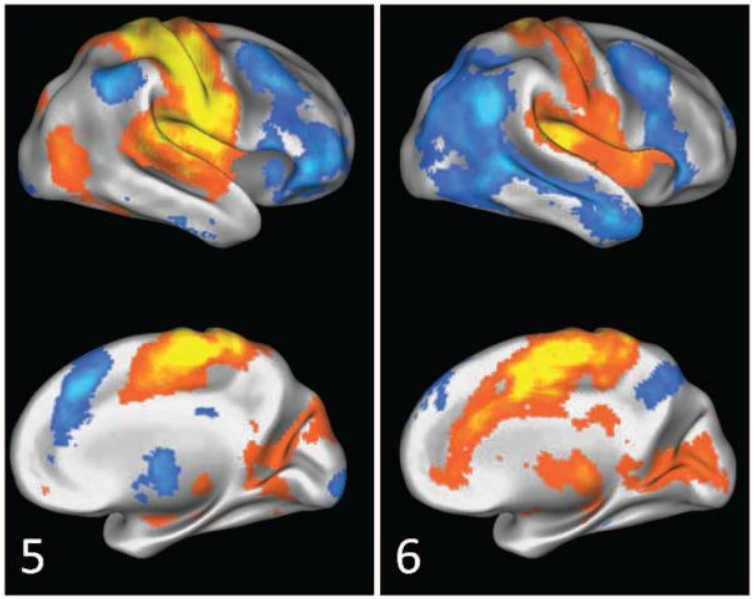

- Visual SCPs

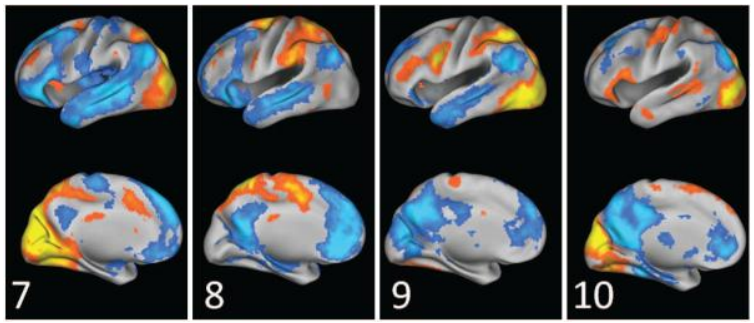

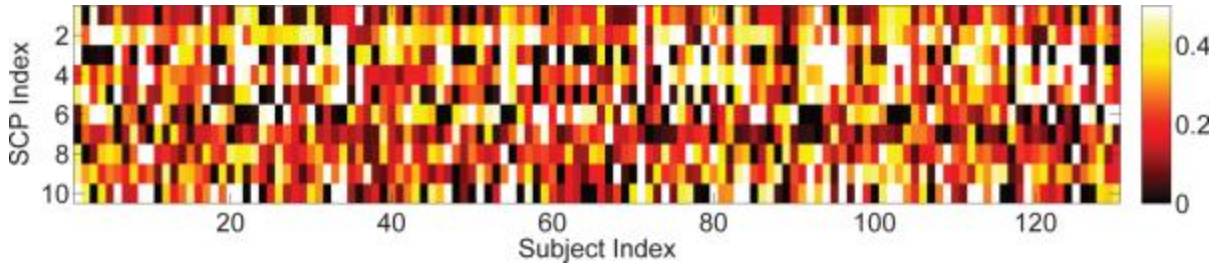

- PCC and the IPL contribute to most of the SCPs, which were identified by a prior study as one of the central hubs of connectivity in the brain.
- Figure 12 shows the strength of presence of each SCP in every subject.

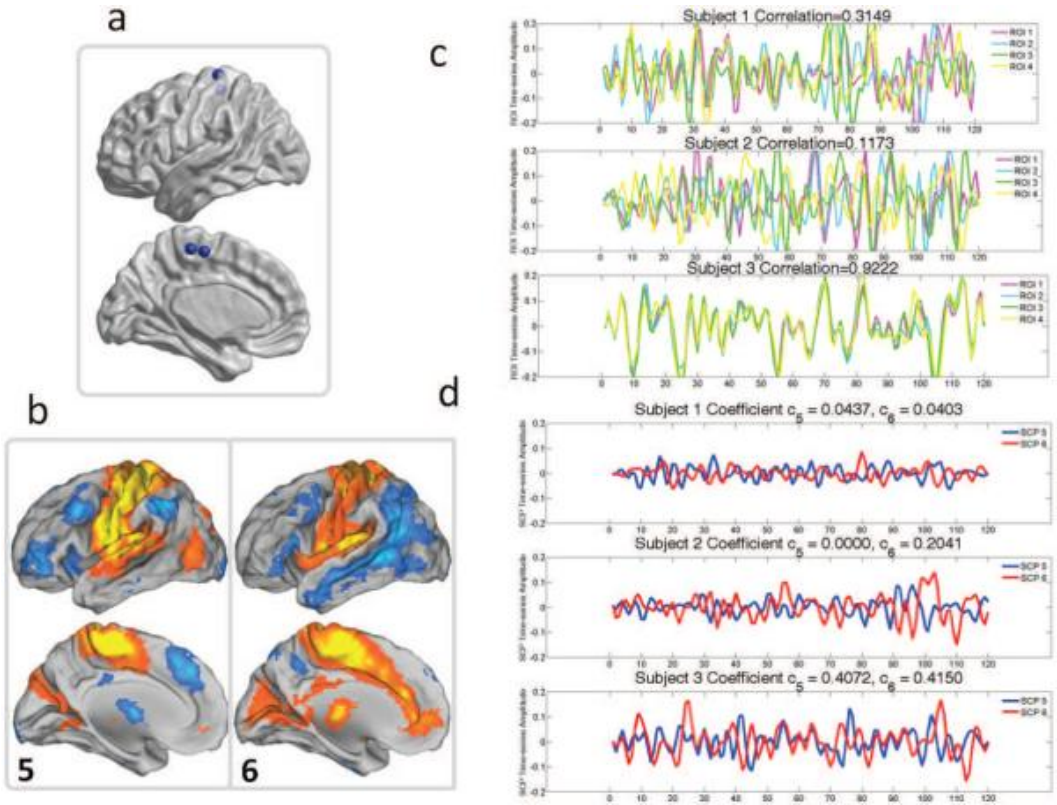

- Inter-subject variability is reflected in the SCP coeffcients.
- Low correlation between the ROIs leads to SCP time-series with very low amplitude.

Reproducibility and Approximation error

- The reproducibility of the SCPs described above is reasonably high.
- Sparse Learning has the best correlation data-fit, while the ICA methods provide the best time-series data fit.

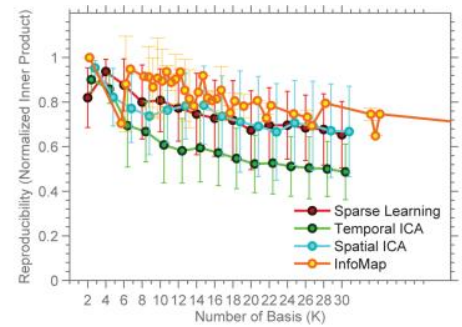

(a) Reproducibility

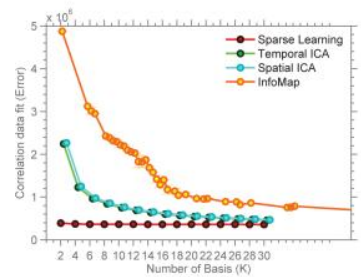

(b) Correlation data-fit (Error)

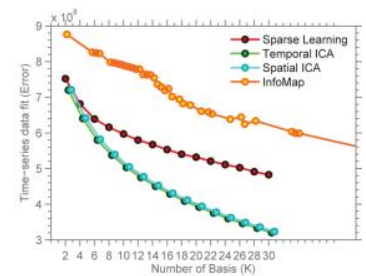

(c) Time-series data-fit (Error)

Spatial Overlap and Temporal Correlation

- InfoMap has no spatial overlap in its basis.
- Spatial ICA shows decreasing overlap with increasing K.
- Sparse Learning has the highest spatial overlap.
- Temporal ICA has no temporal correlation while Spatial ICA has the highest temporal correlation.

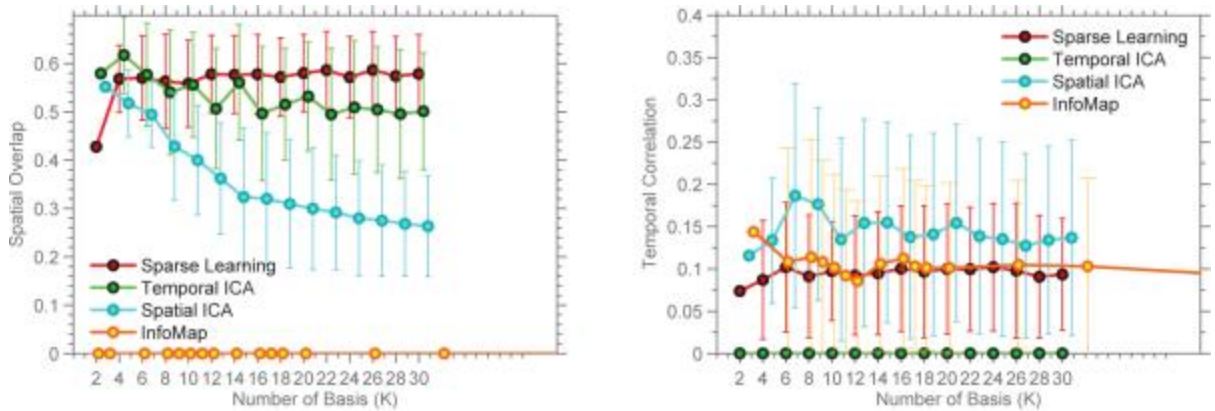

(a) Spatial Overlap (b) Temporal Correlation

Reproducibility across datasets

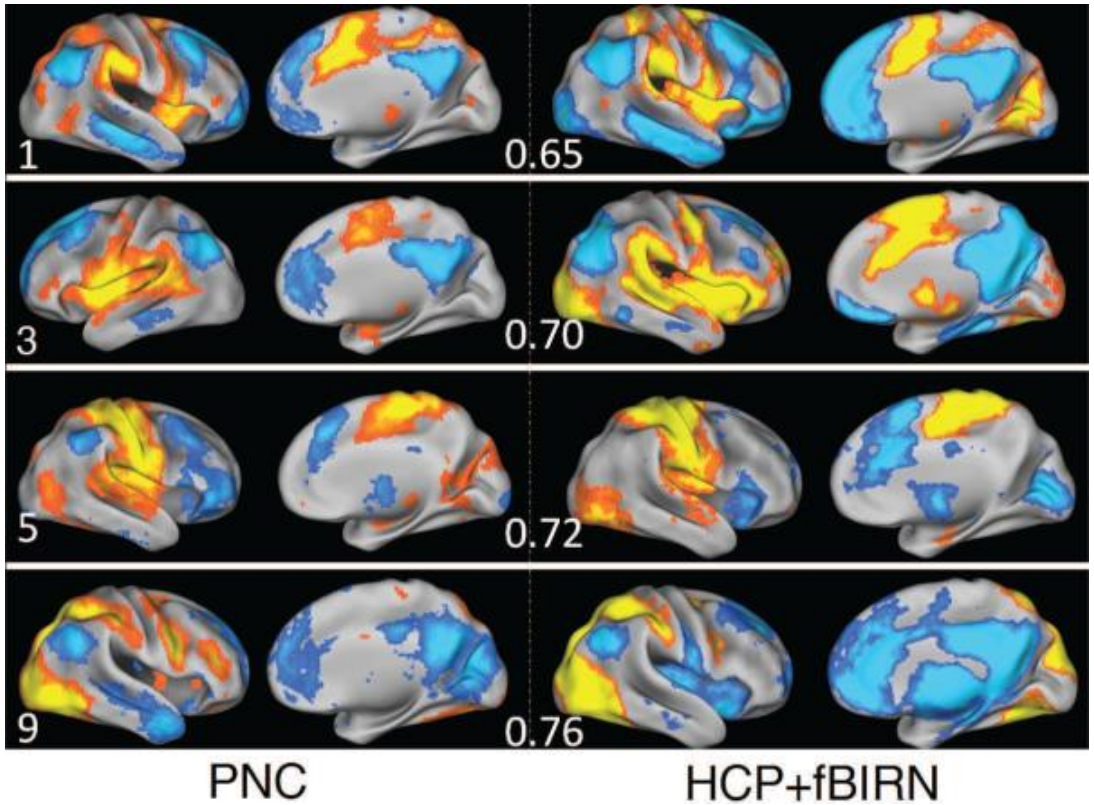

Comparison with sub-graphs and TFMs

- InfoMap assigned major functional systems to different sub-graphs.
- The task-positive regions are assigned to separate sub-graphs.
- All task-negative default-mode regions form a single entity.

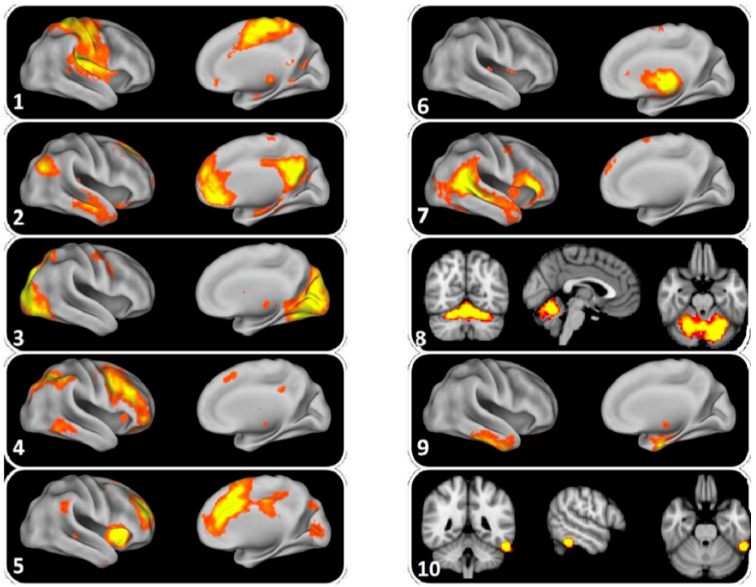

- TFMs identified using ICA are spatially overlapping and incorporate negative values.
- ICA is unable to clearly separate task-positive systems into different components, due to possible temporal co-activation of these systems.

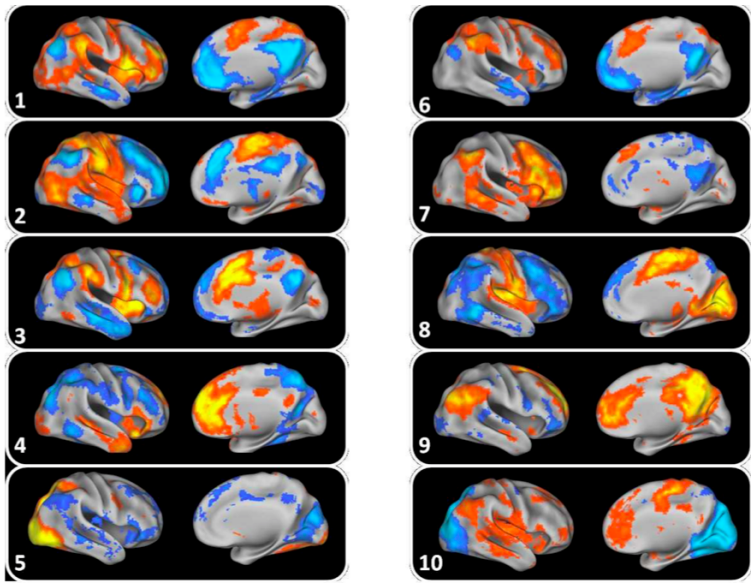

Discussion

- Not all brain regions participate in a given SCP
- Regions that belong to an SCP are functionally coherent, or correlated (or anti-correlated)
- If a set of regions act as an SCP, then, in a set of normal subjects, inter-subject variability is introduced due to the different extent to which each SCP is active in a subject.
- Observations based on simulated experiments
- Interpretation of rsfMRI SCP findings
- Related methods, limitations and future work

Observations based on simulated experiments

- InfoMap and Spatial ICA are able to identify strongly correlated sets of nodes, while avoiding the points of overlap.
- If multiple spatially overlapping networks activate together in some subjects, ICA assigns all these networks to the same TFM.
- if these multiple networks show differential strengths in subjects, the Sparse Learning approach can separate them into different SCPs.

- (Figure 4) When the network sizes are unbalanced, using the same sparsity level λ is inappropriate.
- Picking a value of λ less than size of the largest SCP leads to those SCP getting truncated.
- Picking a value equal to the size of the largest community (= 20% in the simulated case) leads to noisy assignments in the smallest community.
- The sparse decomposition framework adopted herein is a powerful tool for exploring such population heterogeneities.

Interpretation of rsfMRI SCP findings

- SCP is able to separate task-positive regions and their associated task-negative regions into separate SCPs in a data- driven manner, without requiring knowledge of a "seed" region of interest.
- Of greater interest is the differential contribution of regions belonging to the DM within these SCPs (regions in blue).
- (Figure 16) The reproducibility of the SCPs described above is reasonably high.
- InfoMap and Spatial ICA are reliably reproduced, but trading accuracy for greater reproducibility.

Related methods, limitations and future work

- The Sparse Learning approach used herein finds sparse patterns based on second-order statistics (correlation) in each subject's data. PCA and sparse PCA (sPCA) (Moghaddam et al., 2005; d'Aspremont et al., 2008) find directions of maximum variance based on a single covariance matrix common to all data.
- In PCA and sPCA the sparse basis vectors are computed in sequence. The projection of the data along each basis is removed from the data one after one, using **Matrix Deflation**. However, Sparse Learning algorithm, which simultaneously estimates the basis vectors.
- PCA and sPCA maximize the variance $b_k^T \sum b_k$ along the basis direction b_k, which is second-order in the variable bk. The objective function of the proposed method is fourth order in the same variable.

- It is unclear if the high reproducibility of our results reflects true signal, or a systematic artifact induced due to global signal regression.
- Low sample sizes, high dimensionality of the data and large values of K will have a large impact on the stability of the results.
- This framework can also be combined with a discriminative term to obtain functional bio-markers for disease.